Sound & Vibration

Tech Science Press

Multiple Scattering Between Adjacent Sound Sources in Head-Related Transfer Function Measurement System

Guangzheng Yu[1,*], Yu Liu[1,2], Bosun Xie[1] and Huali Zhou[1]

[1]Acoustic Lab., School of Physics and Optoelectronics, South China University of Technology, Guangzhou, 510641, China.

[2]GAC R&D Center, Guangzhou Automobile Group Co., Ltd., Guangzhou, 511458, China.

[*]Corresponding Author: Guangzheng Yu. Email: scgzyu@scut.edu.cn.

Abstract: To accelerate head-related transfer functions (HRTFs) measurement, two or more independent sound sources are usually employed in the measurement system. However, the multiple scattering between adjacent sound sources may influence the accuracy of measurement. On the other hand, the directivity of sound source could induce measurement error. Therefore, a model consisting of two spherical sound sources with approximate omni-directivity and a rigid-spherical head is proposed to evaluate the errors in HRTF measurement caused by multiple scattering between sources. An example of analysis using multipole re-expansion indicates that the error of ipsilateral HRTFs are within the bound of ± 1.0 dB below a frequency of 20 kHz, provided that the sound source radius does not exceed 0.025 m, the source distance relative to head center is not less than 0.5 m, and the angular interval between two adjacent sources is not less than 20 degrees. Similar conclusions under different conditions can also be analyzed and discussed by using this calculation method. Furthermore, the results are verified by measurements of HRTFs for a rigid sphere and a KEMAR artificial head.

Keywords: Head-related transfer function; near field; measurement error; multiple scattering

1 Introduction

Head-related transfer functions (HRTFs) are acoustical transfer functions from a point sound source to two ears in the free field and play an important role in binaural hearing researches and virtual auditory display (VAD). Generally, HRTFs vary with frequency and source position (including azimuth, elevation and distance), and also depend on individual anatomical parameters [1]. When the sound source distance relative to the head center is larger than 1.0 m, HRTFs are approximately independent of source distance and called far-field HRTFs. At a source distance less than 1.0 m, however, HRTFs are relevant to the source distance and called near-field HRTFs [2,3].

Experimental measurement is a common way to acquire individual HRTFs. A conventional measurement system is time-consuming, which usually contains one sound source and the relative position between the sound source and subject is changeable. Alternatively, some systems with two or more sound sources have been employed to accelerate the HRTF measurement [4,5]. However, practical sound sources are not strict point sources, which causes the multiple scattering between the sources or among the sources and head, and thus may result in errors in the measured HRTFs.

In our previous work, the multiple scattering between a single sound source and head in near-field HRTF measurement was evaluated by using a spherical pulsating sound source and a spherical head model [6]. It was suggested that a spherical dodecahedron sound source with radius not more than 0.035 m can be used in the near-field HRTF measurement [7]. In this study, the multiple scattering among two

DOI:10.32604/sv.2019.04644

sound sources and head in HRTF measurement is further analyzed by using the method of multipole reexpansion [8].

2 Calculation Model

In a head-centered coordinate system, the position of a point sound source is specified by vector $\boldsymbol{r}_S$ or spherical coordinate (r_S, α_S, β_S), where r_S is the sound source distance relative to head center, $0^\circ \le \alpha_S \le 180^\circ$ and $0^\circ \le \beta_S < 360^\circ$ are the elevation and azimuth, respectively, with $\alpha_S = 0°, 90°, 180°$ being the above, horizontal and down directions, respectively. In the horizontal plane, $\beta_S = 0°, 90°, 180°$ are front, right and back directions, respectively. Similarly, the position of arbitrary field point is specified by vector $\boldsymbol{r}$ or spherical coordinate (r, α, β). Then, HRTFs are defined as the ratio between the pressure $P(\boldsymbol{r}_{ear}, \boldsymbol{r}_S, f)$ at the left or right ear and the free-field pressure $P_{free}(\boldsymbol{r}_S, f)$ at the position of head center with the head absent.

$$H(\boldsymbol{r}_{ear}, \boldsymbol{r}_S, f) = \frac{P(\boldsymbol{r}_{ear}, \boldsymbol{r}_S, f)}{P_{free}(\boldsymbol{r}_S, f)}, \tag{1}$$

where f denotes the frequency and $\boldsymbol{r}_{ear}$ denotes the ear position $\boldsymbol{r}_L$ or $\boldsymbol{r}_R$. Due to the symmetry of the head, only the right-ear HRTF $H(\boldsymbol{r}_R, \boldsymbol{r}_S, f)$ is analyzed in this paper.

Fig. 1 shows the physical model of HRTF measurement system with two independent sound sources. The model consists of a rigid-spherical head (its center locates at point O_H, and its radius is denoted as a_H) and two spherical sound sources (their centers locate at points O_S and O_T, and their radii are denoted as a_S and a_T, respectively). In practice, the sound sources are driven one by one in the multi-sources measurement system. As a representative case, only the sphere whose center locates at point O_S is an active source which is approximated as a spherical pulsating sound source, and the sphere whose center locates at point O_T serves as a scattering object. Accordingly, in the head-centered coordinate system, the position of O_S is specified by a vector $\boldsymbol{r}_S$ or a spherical coordinate of (r_S, α_S, β_S), and the position of O_T is specified by a vector $\boldsymbol{r}_T$ or a spherical coordinate of (r_T, α_T, β_T).

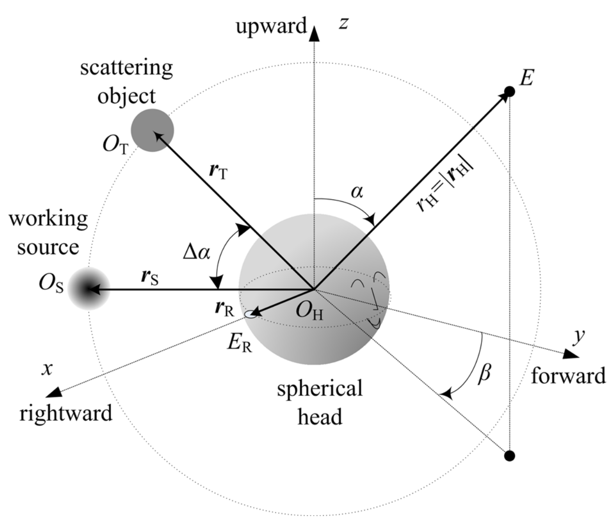

Figure 1: The calculation model and the spatial coordinate system

For the above model, pressure $P(\boldsymbol{r}, \boldsymbol{r}_S, \boldsymbol{r}_T, f)$ satisfies the Helmholtz equation:

$$\nabla^2 P(\boldsymbol{r}, \boldsymbol{r}_S, \boldsymbol{r}_T, f) + k^2 P(\boldsymbol{r}, \boldsymbol{r}_S, \boldsymbol{r}_T, f) = 0, \tag{2}$$

where k is the wave number and ∇^2 is Laplacian operation with respect to the field point $\boldsymbol{r}$. In the infinite distance, the Sommerfeld radiation condition requires,

$$\lim_{r\to\infty} r\left[\frac{\partial P(\boldsymbol{r},\boldsymbol{r}_\mathrm{S},\boldsymbol{r}_\mathrm{T},f)}{\partial r}+\mathrm{j}kP(\boldsymbol{r},\boldsymbol{r}_\mathrm{S},\boldsymbol{r}_\mathrm{T},f)\right]=0\,, \tag{3}$$

where j is the imaginary unit. Assume that the surface S_H of spherical head and the surface S_T of scattering object are rigid, and the normal velocity on the surface S_S of the pulsating sound source is u_S. Then the pressure satisfies the following boundary conditions,

$$\left.\frac{\partial P(\boldsymbol{r},\boldsymbol{r}_\mathrm{S},\boldsymbol{r}_\mathrm{T},f)}{\partial n}\right|_{S_\mathrm{H}}=\left.\frac{\partial P(\boldsymbol{r},\boldsymbol{r}_\mathrm{S},\boldsymbol{r}_\mathrm{T},f)}{\partial n}\right|_{S_\mathrm{T}}=0\quad;\quad\left.\frac{\partial P(\boldsymbol{r},\boldsymbol{r}_\mathrm{S},\boldsymbol{r}_\mathrm{T},f)}{\partial n}\right|_{S_\mathrm{S}}=-2\pi\mathrm{j}\,f\rho u_\mathrm{S}\,, \tag{4}$$

where the symbol $\partial/\partial n$ expresses the derivative with respect to outward normal direction, and the symbol ρ denotes the density of the air.

Generally, the overall sound pressure $P(\boldsymbol{r}, \boldsymbol{r}_\mathrm{S}, \boldsymbol{r}_\mathrm{T}, f)$ consists of four parts, the free-field pressure P_rad radiated by the pulsating sound source, the scattered pressures P_H, P_S and P_T caused by the spherical head, sound source and scattering object, respectively. This leads to

$$P(\boldsymbol{r},\boldsymbol{r}_\mathrm{S},\boldsymbol{r}_\mathrm{T},f)=P_\mathrm{rad}+P_\mathrm{H}+P_\mathrm{S}+P_\mathrm{T}\,. \tag{5}$$

The pressure P_rad can be written as,

$$P_\mathrm{rad}=\mathrm{j}\frac{k\rho cQ_0}{4\pi|\boldsymbol{r}-\boldsymbol{r}_S|}e^{-\mathrm{j}k|\boldsymbol{r}-\boldsymbol{r}_S|}\,, \tag{6}$$

where Q_0 is the source intensity. Within the region of $r < r_\mathrm{S}$, Eq. (6) can be further expanded as

$$\begin{aligned}P_\mathrm{rad}&=\sum_{l=0}^{\infty}\sum_{m=-l}^{l}C_{lm}^\mathrm{H}(k)j_l(kr)Y_{lm}(\alpha,\beta),\\ C_{lm}^\mathrm{H}(k)&=k^2\rho cQ_0\sum_{l=0}^{\infty}\sum_{m=-l}^{l}h_l(kr_\mathrm{S})Y_{lm}^*(\alpha_\mathrm{S},\beta_\mathrm{S})\end{aligned}\,, \tag{7}$$

where $j_l(kr)$ and $h_l(kr_S)$ are the spherical Bessel function and the spherical Hankel function of the second kind, respectively; $Y_{lm}(\alpha_\mathrm{S},\beta_\mathrm{S})$ are the complex-value spherical harmonics functions; superscript "*" denotes complex-conjugate.

The scattering pressure caused by the spherical head can also be expanded as,

$$P_\mathrm{H}=\sum_{l=0}^{\infty}\sum_{m=-l}^{l}A_{lm}^\mathrm{H}(k)h_l(kr)Y_{lm}(\alpha,\beta)\,, \tag{8}$$

where $A_{lm}^\mathrm{H}(k)$ are a set of coefficients to be determined.

To calculate the scattered pressures P_S and P_T, two new coordinate systems are specified. One is centered at the sound source O_S, and the position of arbitrary field point is denoted by (r', α', β'), the other is centered at the scattering object O_T, and the position of arbitrary field point is denoted by (r'', α'', β''). The axes of two new coordinate systems are parallel to the corresponding axes in the head-centered coordinate. In these new coordinate systems, the scattered pressures P_S and P_T can be expanded as

$$\begin{aligned}P_\mathrm{S}&=\sum_{l'=0}^{\infty}\sum_{m'=-l'}^{l'}A_{l'm'}^\mathrm{S}(k)h_{l'}(kr')Y_{l'm'}(\alpha',\beta')\\ P_\mathrm{T}&=\sum_{l''=0}^{\infty}\sum_{m''=-l''}^{l''}A_{l''m''}^\mathrm{T}(k)h_{l''}(kr'')Y_{l''m''}(\alpha'',\beta'')\end{aligned}\,, \tag{9}$$

respectively, where $A_{l'm'}^\mathrm{S}(k)$ and $A_{l''m''}^\mathrm{T}(k)$ are two set of coefficients to be determined.

To apply the boundary condition on the surface S_H of the spherical head, the pressures P_S and P_T should be represented in terms of head-centered coordinate by using following transforming equations

$$h_{l'}(kr')Y_{l'm'}(\alpha',\beta') = \sum_{l=0}^{\infty}\sum_{m=-l}^{l} D_{l'm'lm}^{\mathrm{S}\to\mathrm{H}}(r',\alpha',\beta',r,\alpha,\beta)\, j_l(kr)Y_{lm}(\alpha,\beta)$$
$$h_{l''}(kr')Y_{l''m''}(\alpha'',\beta'') = \sum_{l=0}^{\infty}\sum_{m=-l}^{l} D_{l''m''lm}^{\mathrm{T}\to\mathrm{H}}(r'',\alpha'',\beta'',r,\alpha,\beta)\, j_l(kr)Y_{lm}(\alpha,\beta) \quad , \qquad (10)$$

where $D_{l'm'lm}^{\mathrm{S}\to\mathrm{H}}(k)$ and $D_{l''m''lm}^{\mathrm{T}\to\mathrm{H}}(k)$ are transforming coefficients and determined by the geometrical relationship among coordinates [8]. Substituting Eqs. (5-9) into the boundary condition of surface S_H of the spherical head gives

$$\sum_{l'=0}^{\infty}\sum_{m'=-l'}^{l'} D_{l'm'lm}^{\mathrm{S}\to\mathrm{H}}(k)A_{l'm'}^{\mathrm{S}}(k) + \sum_{l''=0}^{\infty}\sum_{m''=-l''}^{l''} D_{l''m''lm}^{\mathrm{T}\to\mathrm{H}}(k)A_{l''m''}^{\mathrm{T}}(k) + C_{lm}^{\mathrm{H}}(k) = -\frac{h_l'(ka_\mathrm{H})}{j_l'(ka_\mathrm{H})}A_{lm}^{\mathrm{H}}(k) \qquad (11)$$

From the above equation, an infinite set of linear equations with unknown $A_{lm}^{\mathrm{H}}(k)$, $A_{l'm'}^{\mathrm{S}}(k)$ and $A_{l''m''}^{\mathrm{T}}(k)$ can be obtained.

In order to apply the boundary condition on the surface S_S of the sound source and surface S_T of the scattering object, all the pressures P_rad, P_H, P_S and P_T should be represented in terms of sound-source-centered and scattering-object-centered coordinate, respectively. Similar to the schemes above, the other two infinite sets of linear algebra equations with $A_{lm}^{\mathrm{H}}(k)$, $A_{l'm'}^{\mathrm{S}}(k)$ and $A_{l''m''}^{\mathrm{T}}(k)$ as unknown can be obtained by

$$\sum_{l=0}^{\infty}\sum_{m=-l}^{l} D_{lml'm'}^{\mathrm{H}\to\mathrm{S}}A_{lm}^{\mathrm{H}} + \sum_{l''=0}^{\infty}\sum_{m''=-l''}^{l''} D_{l''m''l'm'}^{\mathrm{T}\to\mathrm{S}}A_{l''m''}^{\mathrm{T}} = -\frac{h_l'(ka_\mathrm{S})}{j_l'(ka_\mathrm{S})}A_{l'm'}^{\mathrm{S}}$$
$$\sum_{l'=0}^{\infty}\sum_{m'=-l'}^{l'} D_{l'm'l''m''}^{\mathrm{S}\to\mathrm{T}}A_{l'm'}^{\mathrm{S}} + \sum_{l=0}^{\infty}\sum_{m=-l}^{l} D_{lml''m''}^{\mathrm{H}\to\mathrm{T}}A_{lm}^{\mathrm{H}} + C_{l''m''}^{\mathrm{T}} = -\frac{h_l'(ka_\mathrm{T})}{j_l'(ka_\mathrm{T})}A_{l''m''}^{\mathrm{T}} \quad , \qquad (12)$$

From the three sets of linear algebra equations given by Eqs. (11) and (12), we can solve the coefficients $A_{lm}^{\mathrm{H}}(k)$, $A_{l'm'}^{\mathrm{S}}(k)$ and $A_{l''m''}^{\mathrm{T}}(k)$ by truncating the sets of equations up to order $l \le L-1$. The method for selecting of truncating order is referred to [8]. The overall pressure $P(\boldsymbol{r}, \boldsymbol{r}_\mathrm{S}, \boldsymbol{r}_\mathrm{T}, f)$ at arbitrary field point $\boldsymbol{r}$ (including right ear $\boldsymbol{r} = \boldsymbol{r}_\mathrm{R}$) can be obtained by substituting the obtained coefficients $A_{lm}^{\mathrm{H}}(k)$, $A_{l'm'}^{\mathrm{S}}(k)$ and $A_{l''m''}^{\mathrm{T}}(k)$ into Eq. (5) to Eq. (9). Then the HRTF obtained from the two-source measurement can be estimated from Eq. (1) and denoted by $\hat{H}(\boldsymbol{r}_\mathrm{ear}, \boldsymbol{r}_\mathrm{S}, \boldsymbol{r}_\mathrm{T}, f)$.

In the case of ideal HRTF measurement in which the multiple scattering among the sources and head is neglectable, the HRTF can be calculated by using the analytical solution of the rigid spherical head to the incident wave of a point source and denoted by $H(\boldsymbol{r}_\mathrm{ear}, \boldsymbol{r}_\mathrm{S}, f)$ [9]. Finally, the HRTF magnitude error caused by multiple scattering of sound sources can be evaluated by spectral distortion as

$$SD(r_\mathrm{ear}, \boldsymbol{r}_\mathrm{S}, \boldsymbol{r}_\mathrm{T}, f) = 20\log_{10}\frac{|\hat{H}(\boldsymbol{r}_\mathrm{ear}, \boldsymbol{r}_\mathrm{S}, \boldsymbol{r}_\mathrm{T}, f)|}{|H(\boldsymbol{r}_\mathrm{ear}, \boldsymbol{r}_\mathrm{S}, f)|} \quad (\mathrm{dB})\,. \qquad (13)$$

3 Calculation Results

Suppose that head radius is a_H = 0.0875 m [9], and both spherical source and scattering object locate at the same distance and azimuth, namely, $r_\mathrm{S} = r_\mathrm{T}$ and $\beta_\mathrm{S} = \beta_\mathrm{T}$, but at various elevations with elevation interval of $\Delta\alpha = \alpha_\mathrm{S} - \alpha_\mathrm{T}$. Fig. 2 shows a simple example of calculation. Fig. 2(a) illustrates the calculation conditions, namely the source distance is 0.5 m, the radius of the spherical source is 0.025 m, and the elevation interval is 25°. Fig. 2(b) shows the spectral distortion *SD* evaluated from Eq. (13). The prominent errors mainly appear at the source azimuths which are contralateral to the concerned ear (within $225° \le \beta_\mathrm{S} < 315°$ for the right ear). The *SD* reaches up to about 10.0 dB at high frequencies above about 7 kHz. However, because the high-frequency HRTF magnitude for contralateral source directions is naturally small due to the shadow of head, its contribution to auditory perception is relatively minor. The error in contralateral HRTF magnitude at high frequency is tolerable. In contrast, the errors in the other azimuths are small and *SD* varies within the bound of about ± 1.0 dB in the whole audible frequency band, which satisfies the requirement of HRTF measurement [1].

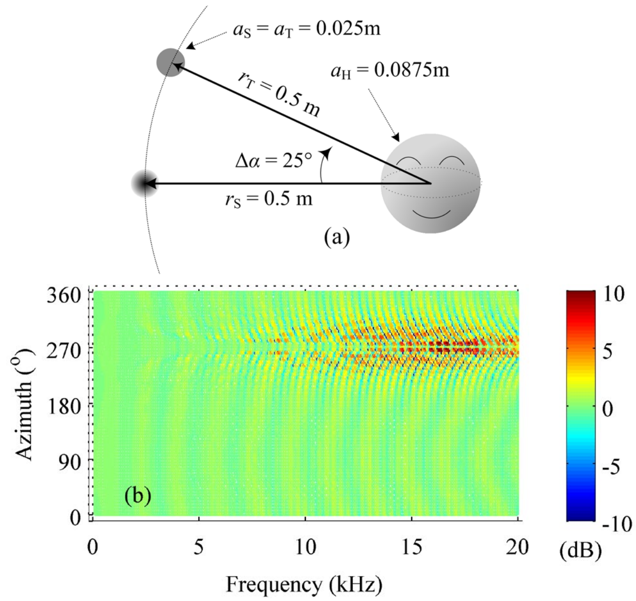

Figure 2: (a) The conditions of a calculation example; (b) the errors of the calculated right ear HRTFs at various azimuths

Accordingly the error at an arbitrary ipsilateral azimuth, for instance the horizontal azimuth of β_S = 90°, can be seen as the representative one. Therefore, in the following discussions, only the HRTF errors at azimuth β_S = 90° are calculated and analyzed. Under the conditions of (β_S = 90° and a_H = 0.0875 m), the errors depend on the spherical source radius ($a_S = a_T$), the source distance ($r_S = r_T$), and the angle interval $\Delta\alpha$ between the two sources.

At the source distance of 0.5 m, the HRTF errors as defined in Eq. (13) with source elevation intervals of 15°, 20° and 25° are shown in Fig 3. Results show that the errors increase as the source elevation interval decreases. For the elevation interval of 15°, the errors reach up to about ± 1.5 dB at several frequencies. In the multi-sources HRTF measurement system, if the acceptable limit of error is ± 1.0 dB, the elevation interval should not less than 20° at the distance of 0.5 m.

In the case of the elevation interval of 20°, the HRTF errors at source distances of 0.2 m, 0.5 m, and 1.0 m are shown in Fig. 4. Results indicate that the errors increase as the source distance decreases and reach up to ± 2.5 dB at source distance 0.2 m. On the other hand, the errors at 1.0 m are only within the bound of ± 0.5 dB. Therefore, for the sources in far field (source distance not less than 1.0 m), the permitted elevation interval could be smaller and the allowable sizes of sound sources could be larger.

As shown in Fig. 5, at source distance of 1.0 m and under the error criterion of ± 1.0 dB, the elevation interval can be decreased to 10° and the source radius can be enlarged to 0.035 m. However, the errors further increase as the spherical source radius increase. For the source radius 0.05 m and the elevation interval 10°, the HRTF errors reach up to about ± 2.0 dB, which is unacceptable in HRTF measurement. Above results yield the reasonable conditions of multi-sources measurement system for near-field and far-field HRTFs.

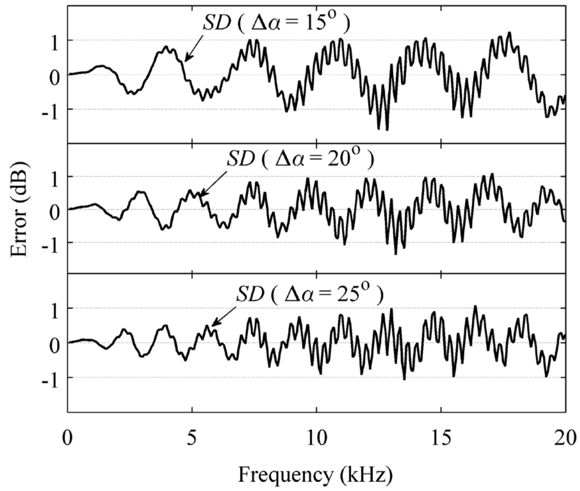

Figure 3: The HRTF errors for the elevation intervals of 15°, 20° and 25°, the source distance of 0.5 m, the spherical source radius of 0.025 m, and the sound source azimuth of β_S = 90°

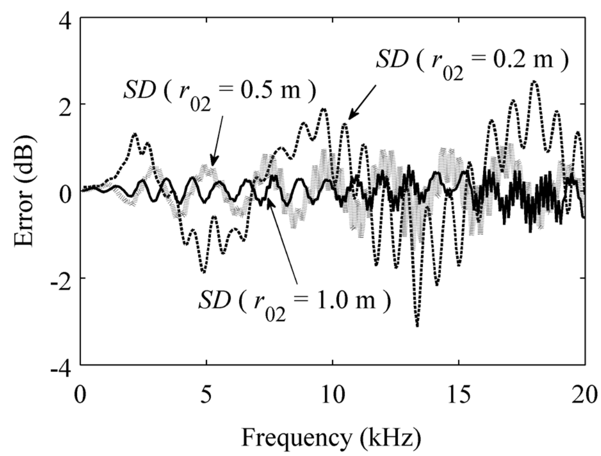

Figure 4: For the spherical source radius of 0.025 m, the elevation interval of 20°, and the sound source azimuth of β_S = 90°, the errors at source distances ($r_S = r_T$) of 0.2 m, 0.5 m and 1.0 m

4 Validation via Measurement

In order to validate the results, we design two spherical dodecahedron sound sources with radius of about 0.025 m and a woody spherical head model with radius of about 0.0875 m, and then the HRTFs of the head model are measured by using two sound sources and denoted by $\hat{H}(\boldsymbol{r}_{ear}, \boldsymbol{r}_S, \boldsymbol{r}_T, f)$. Fig. 6(a) shows the configuration of head model and sound sources, which is identical that shown in Fig. 2(a). Removing the spherical source O_T, the measured HRTFs can be deemed as the accurate ones and denoted by $H(\boldsymbol{r}_{ear}, \boldsymbol{r}_S, f)$. Fig. 6(b) shows the errors of the measured HRTFs defined by Eq. (13).

In comparison with the calculated results in Fig. 2(b), some discrepancies are observed in Fig. 6(b), but only at high frequencies and the contralateral azimuths. It is interesting to observe that some prominent errors predicted by calculation disappear in the measured results. Actually, the interferences of sound wave from various paths around a perfect rigid-spherical head make the contralateral HRTFs very sensitive to the small disturbance. A slight multiple scattering from sound sources may cause a large change in the contralateral HRTF magnitudes. The woody spherical-head model is not as perfect as the theoretical one, which weakens the influence of interferences of sound wave at the contralateral ear and makes the corresponding HRTFs less sensitive to the small disturbance. For the human subjects, the head shape is more irregular than a spherical head, which could further decrease the contralateral errors in HRTF measurement. In other words, the error in practical HRTF measurement at contralateral directions may be overestimated by the calculation model shown in Fig. 2(a). This is beneficial to practical design of measurement system.

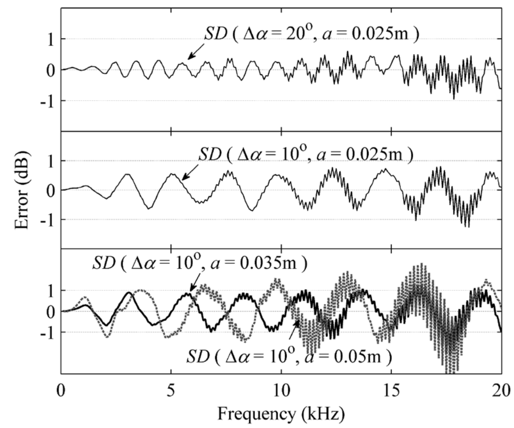

Figure 5: The HRTF errors at the azimuth $\beta_S = 90°$ and the source distance 1.0 m, the spherical source radii are 0.025 m, 0.35 m and 0.05 m, and the elevation intervals include 10° and 20°, respectively

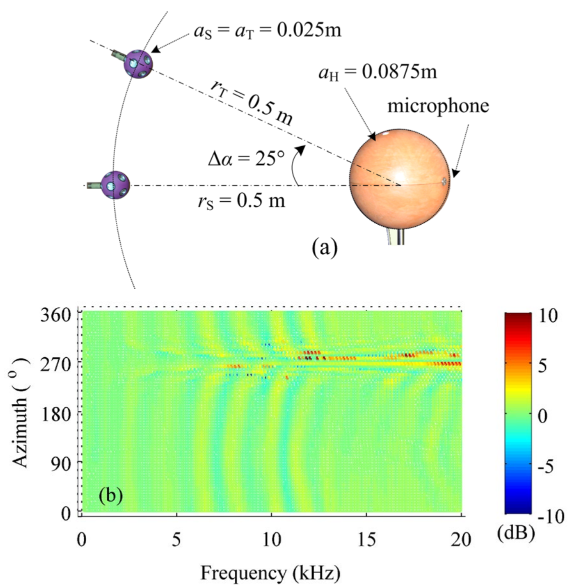

Figure 6: (a) The conditions of HRTF measurement; (b) the errors of the measured HRTFs at various azimuths

To verify the above-mentioned hypothesis, paying attention to the magnitude error less than 2.5 dB at distance 0.2 m in Fig. 4, 4 sound sources are set at distance 0.2 m with elevations (α = -30°, 0°, 30°, 60°, respectively) in the near-field HRTF measurement for a KEMAR artificial head. The results are shown in Fig. 7. Errors of most azimuths fall within about 1.0 dB when multiple sound sources are deployed. The errors reach up to or beyond 2.0 dB only when the sound sources are located at the contralateral side (β = 270°). This is because, as mentioned previously in this paper, the multiple scattering sound waves among sources have greater influence on contralateral HRTF with small amplitude. With the increase of source distance, the spatial interval among sources get larger and the scattering errors will decrease further. This indicated that the above-mentioned spherical dodecahedron sound source is suitable for multiple-sound-source HRTF measurement system.

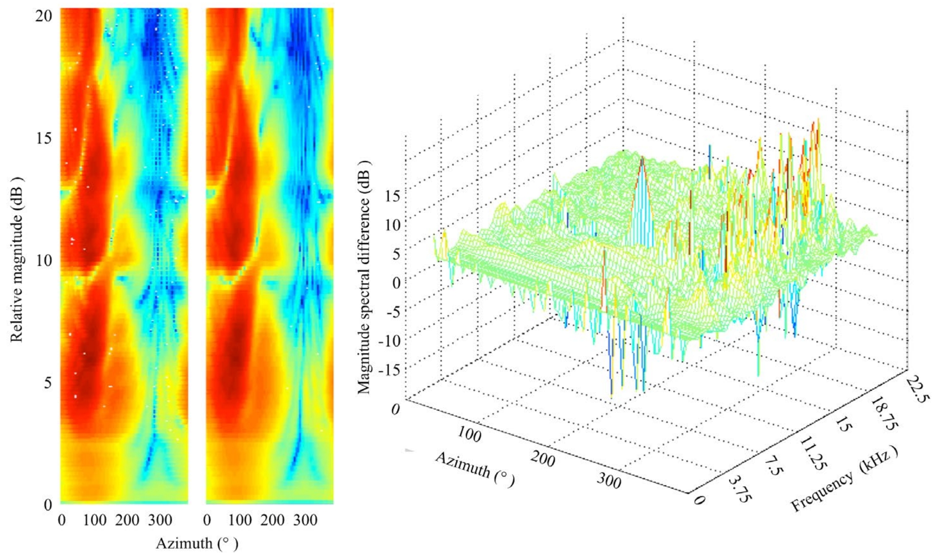

Figure 7: Influence of multiple-sound-source scattering to near-field HRTF measurement using a KEMAR artificial head. (a) the right-ear HRTF measured with deployment of multiple sound sources; (b) the right-ear HRTF measured with deployment of a single sound source; (c) magnitude spectral difference (*SD* in dB)

5 Conclusions

The model consisting of a rigid spherical head and two spherical sound sources has been used to analyse the errors in HRTF measurements caused by multiple scattering of the adjacent sound sources. The errors increase with the increasement of the source radius and the decrement of the source distance and elevation interval. Especially, the spectral distortion in ipsilateral HRTF measurement are within ± 1.0 dB for the frequencies below 20 kHz, source radius less than 0.025 m, source distance not less than 0.5 m, and the elevation interval of the adjacent sources not less than 20°. Using similar method, the cases of various sound source distances and intervals can be analyzed. The measurement results of the multiple scattering of the rigid spherical head model and a KEMAR manikin further verified the calculation results. In practice, some sound absorption treatments on the source surface can further reduce the error caused by multiple scattering, and thus further improve the accuracy of measurement.

Acknowledgments: This work was funded by National Natural Science Foundation of China (No. 11574090) and Natural Science Foundation of Guangdong Province (No. 2018B030311025).

References

1. Xie, B. S. (2013): *Head related transfer function and virtual auditory display (second edition)*. J Ross Publishing, USA.
2. Yu, G. Z., Wu, R. X., Liu, Y., Xie, B. S. (2018): Near-field head-related transfer-function measurement and database of human subjects. *Journal of the Acoustical Society of America, 143(3),* 194-198.
3. Brungart, D. S., Rabinowitz, W. M. (1999): Auditory localization of nearby sources. Head-related transfer functions. *Journal of the Acoustical Society of America*, *106(3),* 1465-1479.
4. Begault, D. R., Godfroy, M., Miller J. D., Roginska, A., Anderson, M. R. et al. (2006): Design and verification of HeadZap, a semi-automated HRIR measurement system. *AES 120th Convention*.
5. Pollow, M., Masiero, B., Dietrich, P., Fels, J., Vorländer, M. (2013): Fast measurement system for spatially continuous individual HRTFs. *AES 25th UK Conference*.
6. Yu, G. Z., Xie, B. S., Rao, D. (2008): Effect of sound source scattering on measurement of near-field head-

related transfer functions. *Chinese Physics Letters, 25(8),* 2926-2929.

7. Yu, G. Z., Xie, B. S., Rao, D. (2010): Directivity of spherical polyhedron sound source used in near-field HRTF measurements. *Chinese Physics Letters, 27(12),* 124302-124302.
8. Gumerov, N. A., Duraiswami, R. (2002): Computation of scattering from N spheres using multipole reexpansion. *Journal of the Acoustical Society of America, 112(6),* 2688-2701.
9. Duda, R. O., Martens, W. L, (1998): Range dependence of the response of a spherical head model. *Journal of the Acoustical Society of America, 104(5),* 3048-3058.